IOP Publishing Journal of Physics: Condensed Matter

J. Phys.: Condens. Matter **23** (2011) 194101 (10pp) doi:10.1088/0953-8984/23/19/194101

How much does the core structure of a three-phase contact line contribute to the line tension near a wetting transition?

J O Indekeu[1], K Koga[2] and B Widom[3]

[1] Institute for Theoretical Physics, Katholieke Universiteit Leuven, BE-3001 Leuven, Belgium
[2] Department of Chemistry, Faculty of Science, Okayama University, Okayama 700-8530, Japan
[3] Department of Chemistry, Baker Laboratory, Cornell University, Ithaca, NY 14853-1301, USA

Received 27 September 2010, in final form 21 November 2010
Published 27 April 2011
Online at stacks.iop.org/JPhysCM/23/194101

Abstract

We initially simplify a three-phase contact line to a 'primitive' star-shaped structure formed by three planar interfaces meeting at a common line of intersection, and calculate the line tension associated with this primitive picture. Next, we consider the well-known more refined picture of the contact line that includes a 'core structure' consisting of interface deviations away from the planar interface picture. The corresponding contact line properties were calculated earlier, within mean-field theory, using an interface displacement model or a more microscopic density-functional theory. The question we ask is to what extent the thermodynamic line tension of the contact line near a wetting phase transition can be attributed to the core structure. To answer it we compare our result for the line tension contribution associated with the primitive structure to the known line tension of the full structure (within mean-field theory). While our primitive structure calculation provides a surprisingly useful upper bound to the known line tension near a critical wetting transition, the nontrivial core structure of the contact line near first-order wetting is found to be responsible for an important difference between the known line tension and the upper bound provided by the primitive picture calculation. This accounts also for the discrepancy between the line tensions calculated by two different methods in an earlier mean-field density-functional model of a first-order wetting transition.

Dedicated to Henk Lekkerkerker on the occasion of his 65th birthday

1. Prelude

Interfacial phenomena, and wetting in particular, have been notable subjects of Henk Lekkerkerker's research interests for a long time and to this day [1]. The fate of the line tension [2] in the vicinity of the surface phase transition from partial to complete wetting [3] is a fundamental problem, which has enjoyed his special attention for many years. The behavior of the three-phase contact line at wetting displays the full physics of phase transitions and critical phenomena, including universal and non-universal aspects. Particularly intriguing is that the order of the wetting transition and the range of the intermolecular forces are all-important for determining the sign, magnitude and critical singularity of the line tension. Our understanding of the three-phase contact line and its tension has considerably deepened and sharpened over the last three decades [4–8]. A tutorial recapitulation of the main prerequisites relevant to our study is included in [9]. The essentials will be recalled here.

What happens to the contact line, and to its excess free energy per unit length, the line tension τ, when the thermodynamic contact angle θ approaches zero? In 1992 a study based on a simple interface displacement model (IDM) predicted that for first-order wetting the contact line does not disappear at wetting, but becomes an extended transition zone connecting a thin adsorbed film to a macroscopic wetting layer [10]. Consequently, τ does not vanish. On the other hand, for critical wetting the contact line gradually disappears, and its tension vanishes, as the adsorbed film thickness diverges in a continuous manner for $\theta \to 0$. Further, intermolecular van der

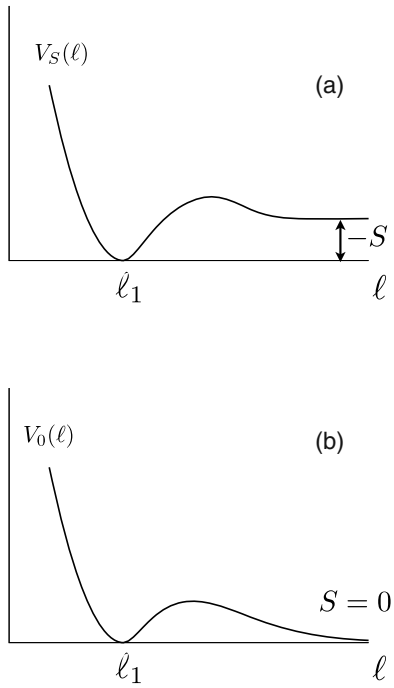

Figure 1. (a) Interface potential for a partial wetting state anticipating a first-order wetting transition. The equilibrium thin film has thickness ℓ_1 and the spreading coefficient S is negative. (b) Interface potential at a first-order wetting transition. The equilibrium thin film has thickness ℓ_1 and coexists with a macroscopic wetting layer of infinite thickness. The spreading coefficient is zero.

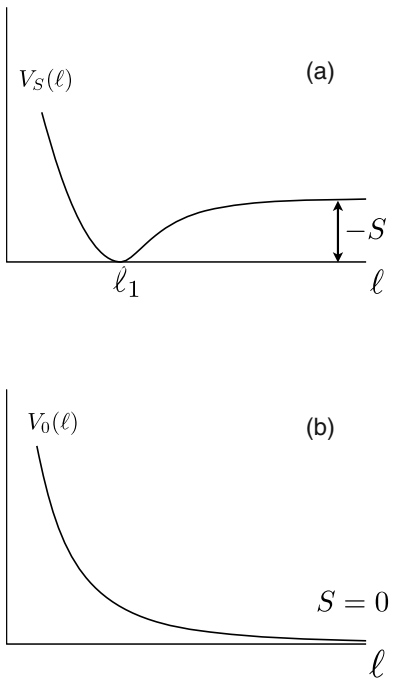

Figure 2. (a) Interface potential for a partial wetting state anticipating a critical wetting transition. The equilibrium thin film has thickness ℓ_1 and the spreading coefficient S is negative. (b) Interface potential at a critical wetting transition. The equilibrium film is a wetting layer of infinite thickness. The spreading coefficient is zero.

Waals forces lead to different behavior for τ than short-range forces (of finite range or exponential decay). For example, for first-order wetting and non-retarded van der Waals forces, τ diverges at wetting, in the manner $\tau(\theta) \propto \log(1/\theta)$, while for short-range forces τ reaches a finite positive value $\tau(0)$. For critical wetting and non-retarded van der Waals forces, $\tau(\theta) \leqslant 0$ and τ vanishes at wetting, in the manner $\tau(\theta) \propto -\theta^{1/3}$, while for short-range forces $\tau(\theta) \propto -\theta$ [10]. In line with expectations [11] the quantitative predictions of the IDM are in excellent agreement with accurate computations based on a more microscopic density-functional theory with two spatially varying order parameters [4].

We now recall the mean-field theory embodied in the IDM. The line tension $\hat{\tau}[\ell]$ is the following functional of the interface displacement $\ell(x)$, with x the coordinate parallel to the substrate plane and perpendicular to the contact line [10, 12]:

$$\hat{\tau}[\ell] = \int_{-\infty}^{\infty} \mathrm{d}x \left\{ \gamma \left(\sqrt{1 + \left(\frac{\mathrm{d}\ell}{\mathrm{d}x} \right)^2} - 1 \right) + V(\ell(x)) + c(x) \right\}. \tag{1}$$

Firstly, this functional features the free energy cost, per unit length of the contact line, of interface distortions which increase the interfacial area relative to that of a flat plane. This cost is proportional to the (liquid–vapor) interfacial tension γ and the increment $\mathrm{d}s - \mathrm{d}x$, with $\mathrm{d}s^2 = \mathrm{d}\ell^2 + \mathrm{d}x^2$. The second contribution concerns the free energy cost of imposing an arbitrary interface displacement ℓ. For a uniform ℓ, independent of x, this cost is given by an interface potential $V(\ell)$, per unit area. This $V(\ell)$ is the constrained surface free energy of an adsorbed film of imposed thickness ℓ. Typical examples of interface potentials are shown in figure 1 in the context of first-order wetting and in figure 2 in the context of critical wetting. The minimum of $V(\ell)$ is reached for the equilibrium thickness of the adsorbed film, which we denote by ℓ_1. For partial wetting, ℓ_1 is finite, while for complete wetting the minimum lies at $\ell = \infty$. A first-order wetting transition corresponds to an interface potential with two equal minima, one at $\ell = \ell_1$ and one at $\ell = \infty$, separated by a free energy barrier (figure 1(b)). A critical wetting transition corresponds to an interface potential without barrier and with a single minimum, which continuously moves out to infinity, $\ell_1 \to \infty$, for $\theta \to 0$ (figure 2(b)).

We adopt the local approximation and extend this free energy to non-uniform displacements by replacing ℓ by $\ell(x)$ in the argument of V. A piecewise constant function $c(x)$ is added to ensure that the integrand approaches zero smoothly in the two limits, $x \to -\infty$, where the displacement reaches the value ℓ_1 in the thin equilibrium adsorbed film, and $x \to \infty$, where the displacement assumes the slope $\mathrm{d}l/\mathrm{d}x \sim \tan\theta$ appropriate for a liquid wedge with contact angle θ. By virtue of $c(x)$, the model features an intrinsic dividing line, at $x = x_\mathrm{d}$, where the asymptotic planar configurations intersect. Without loss of generality we can take $x_\mathrm{d} = 0$. For more details, we refer the reader to [10].

For our purposes we consider $\mathrm{d}\ell/\mathrm{d}x$ small and linearize the functional in the squared gradient. Minimization of $\hat{\tau}[\ell]$ is then equivalent to finding least action trajectories for a particle

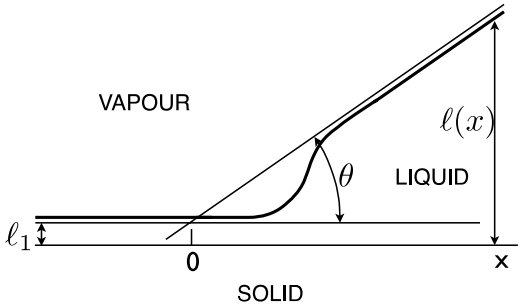

Figure 3. Interface displacement profile for partial wetting, anticipating a first-order wetting transition, after [10].

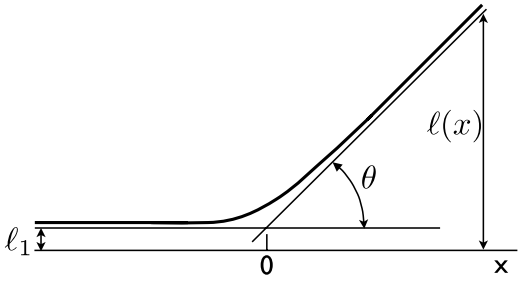

Figure 4. Interface displacement profile for partial wetting, anticipating a critical wetting transition, after [10].

with position ℓ at time x, moving in a potential $-V$. The Euler–Lagrange equation,

$$\gamma \frac{\mathrm{d}^2\ell}{\mathrm{d}x^2} = \frac{\mathrm{d}V}{\mathrm{d}\ell}, \tag{2}$$

is to be solved with boundary conditions $\ell \to \ell_1$ for $x \to -\infty$, and $\ell \to (\tan\theta)x \approx \theta x$, for $x \to \infty$. By convention we choose $V(\ell_1) = 0$, so that $V(\infty) = -S$, $S \leqslant 0$ being the so-called spreading coefficient, which is the excess free energy of a macroscopic wetting layer relative to that of the equilibrium film. With $-S = \gamma(1 - \cos\theta) \approx \gamma\theta^2/2$, the 'constant of the motion'

$$\frac{\gamma}{2}\left(\frac{\mathrm{d}\ell}{\mathrm{d}x}\right)^2 - V(\ell) = 0 \tag{3}$$

is satisfied by the optimal profile $\ell(x)$. In the mechanical analogy the particle moves with zero total energy and with velocity proportional to $\sqrt{V(\ell(x))}$. We show the resulting interface displacement profiles for a partial wetting state near a first-order wetting transition in figure 3, for which $\ell(x)$ displays an S-shape due to the barrier in $V(\ell)$, and for a partial wetting state near a critical wetting transition in figure 4, for which the slope of $\ell(x)$ is monotonic.

The equilibrium line tension has the value $\hat{\tau}[\ell]$ for the optimal profile, and is given by

$$\tau(S) = \sqrt{2\gamma}\int_{\ell_1}^{\infty} \mathrm{d}\ell \left\{\sqrt{V(\ell)} - \sqrt{-S}\right\}. \tag{4}$$

The value $\tau(0)$ is proportional to the integral over the square root of the barrier in $V(\ell)$, for first-order wetting, or equals zero, for critical wetting, provided $\sqrt{V(\ell)}$ is integrable for large ℓ. For a d-dimensional bulk system with intermolecular pair potentials $\phi(r)$, which for large intermolecular distance r decay as

$$\phi(r) \propto r^{-(d+\sigma)}, \tag{5}$$

the interface potential decays as [13]

$$V(\ell) \propto \ell^{-(\sigma-1)}. \tag{6}$$

Here, σ is a number which depends on the system under consideration. For example, $\sigma = 3$ (4) for non-retarded (retarded) van der Waals forces in $d = 3$. Clearly, whether or not the line tension diverges depends on the tail of $V(\ell)$. A similar observation was made by de Feyter and Vrij [14] who studied borders of thin soap films.

The IDM predicts that the line tension diverges, already for non-zero S, if $\sigma \leqslant 2$. This can be seen by expanding $\sqrt{V}$ in the integrand of (4) about $\sqrt{-S}$, for large ℓ, and is not unexpected since bulk energy densities diverge for $\sigma \leqslant 0$ and interfacial tensions diverge for $\sigma \leqslant 1$. In order for the thermodynamic limit of excess quantities to exist, the forces must be of sufficiently short range. Further, for first-order wetting (i.e., when a barrier in $V(\ell)$ persists), the line tension reaches a finite and positive limit provided $\sigma > 3$ and diverges for $\sigma \leqslant 3$. A possible divergence of $\tau(0)$ for non-retarded van der Waals forces was anticipated by Joanny and de Gennes in 1986 [17]. However, for critical wetting, $\tau(0) = 0$ for van der Waals forces. In fact, $\tau(\theta) \propto -\theta^{(\sigma-2)/\sigma}$ for $\theta \to 0$ and for $\sigma > 2$ [10].

2. Motivation

A schematic drawing à la Gibbs (figure 5(a)) shows a primitive picture of a three-phase contact line consisting of the junction of three planar interfaces ('when (...) three surfaces of discontinuity (...) meet along a line' [15]). In reality a core structure is present, which to a first approximation can be visualized as interface deviations away from the planar interface picture [16]. In figure 5(a) this core structure is neglected; only the asymptotic structure, consisting of the planar interfaces far from the contact line, has been respected and the location of the planes has been adjusted so that they have a single common line of intersection. We can now ask what is the line tension corresponding to this 'primitive' picture of the contact line, and how does it differ from the improved estimate which results if interface deviations close to the contact line are taken into account (figures 5(b) and (c)). In other words, we ask which contribution to the line tension comes from the mere presence of the contact line with associated dihedral angles but without core structure, and which contribution is due to the core structure represented by interface deviations away from simple intersecting planes.

Are these questions interesting? We know that, depending on the order of the wetting transition and the range of the forces, the mean-field theory predicts that the line tension at wetting can be zero, positive and finite, or positive infinity. Our present investigation aims at revealing which aspects of the geometrical contact line structure are responsible for these

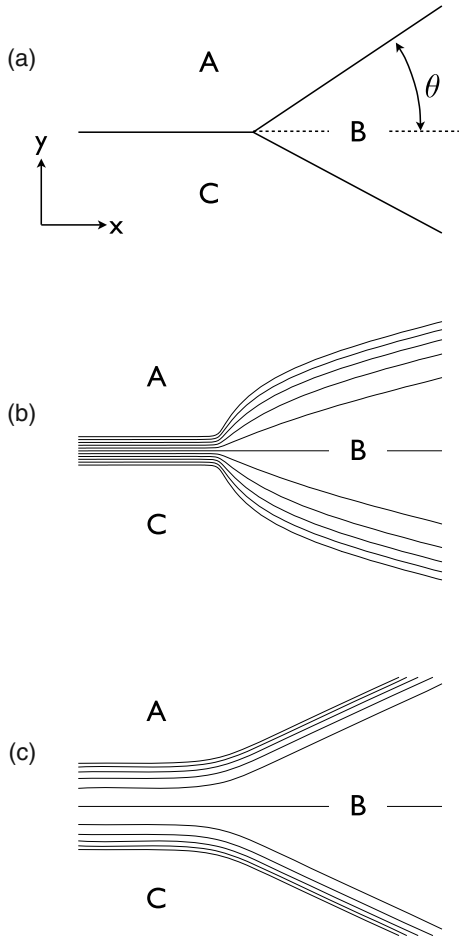

Figure 5. Equilibrium configurations of a contact line where three coexisting phases A, B and C and their mutual interfaces meet. (a) A primitive picture of a three-phase contact line. (b) A more refined picture of a three-phase contact line with a core structure appropriate for the approach to a first-order wetting transition. The core structure was computed using the density-functional model of the first paper of [4]. Contour plots are shown of one of the densities, $\rho_1(x, y)$, featuring in that model. (c) A more refined picture of a three-phase contact line, with a core structure appropriate for the approach to a critical wetting transition. The core structure was computed using the density-functional model of the second paper of [4]. Contour plots are shown of one of the densities, $\rho_1(x, y)$, featuring in that model.

outcomes. For example, we know that $\tau(0)$ is positive and finite at first-order wetting for short-range forces. Is part of this finite value attributable to the primitive configuration and another to the core structure of the contact line? Is the part that arises from the core structure a (small) correction? We will discover shortly that, interestingly, the answer is 'no' to both questions. However, if the wetting transition is critical, the answer to both is 'yes'. Therefore, in hindsight we can conclude that the questions we pose are interesting because the answers are surprising and lead to new insight. We will employ the IDM to obtain precise analytic answers within mean-field theory. For first-order wetting, complementary numerical results will be obtained from the more microscopic density-functional theory with two spatially varying densities.

A second motivation, besides investigating the influence of geometrical contact line structure on the line tension, is to

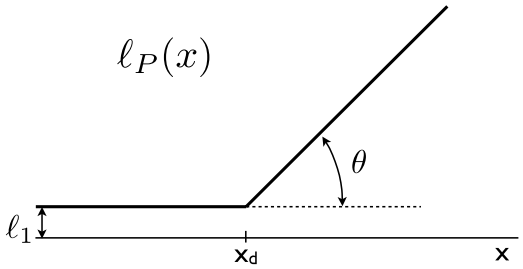

Figure 6. Primitive interface displacement profile $\ell_P(x)$ consisting of a piecewise linear function. The thickness of the equilibrium film is ℓ_1. The contact angle is θ and the dividing line is located at $x = x_d$.

test the quality of a simple upper bound to the line tension, derived by restricting the interface displacement profiles in the IDM to the set of piecewise linear functions $\ell(x)$ (figure 6). These functions would optimize the line tension functional if the interface potential $V(\ell)$ were negligible. Clearly, these piecewise linear trial functions correspond to the primitive configuration discussed before (figure 5(a)). Is the upper bound to the line tension obtained in this way useful? Is its value close to that which follows from solving the full variational problem? We shall uncover that, again, the answer depends crucially on the order of the wetting transition. Within the IDM we can obtain exact results which shed light on these questions.

A third and final motivation for our present study starts with the observation that the primitive (piecewise linear) interface displacement profile (figure 6) is uniquely determined by specifying the value of the contact angle and the value of the equilibrium film thickness ℓ_1. The shape of the primitive profile (a simple corner) does not distinguish between first-order wetting or critical wetting. The more relaxed profiles which satisfy the Euler–Lagrange equation (2), in contrast, are much more sensitive to the order of the transition. The distinction, conspicuous in the optimal profiles (figures 3 and 4), is due to the presence of an interface potential barrier separating two equal minima (first-order wetting) or the absence of a barrier and existence of a single minimum (critical wetting). The primitive profiles only depend on the order of the wetting transition through the asymptotic behavior of ℓ_1 (recall that ℓ_1 remains small for first-order wetting but diverges for critical wetting). We can therefore now ask how the associated line tension depends on whether two minima of the interface potential are involved in the transition zone or only one, using the primitive profile instead of the optimal ones. Surprisingly, although the asymptotic primitive profile, for $\theta \to 0$, is characterized by a vanishing derivative $\mathrm{d}\ell/\mathrm{d}x$ for all x for both cases, we will find that the respective line tensions can differ by an infinite amount! The difference is more important than for the optimal profiles.

3. Results

3.1. Preliminary remarks concerning the line tension

The primitive profile $\ell_P(x)$ displays an intrinsic dividing line at $x = x_d$ (see figure 6). Following (4.10) in [10] we write, for

small θ, and in the gradient-squared approximation,

$$\hat{\tau}[\ell] = \int_{-\infty}^{\infty} \mathrm{d}x \left\{ \frac{1}{2}\gamma \left(\frac{\mathrm{d}\ell}{\mathrm{d}x} \right)^2 + V_S(\ell(x)) - \Theta(x - x_\mathrm{d})[\gamma_\mathrm{sl} - \gamma_\mathrm{sv} + \gamma/\cos\theta] \right\}. \quad (7)$$

From now on we include the subscript S in V_S, which refers to the spreading coefficient. Further, γ_sl and γ_sv stand for the solid–liquid and solid–vapor surface free energies in the concrete case of a solid substrate and an adsorbate at liquid–vapor two-phase coexistence, but one may generalize this picture to describe any equilibrium of three phases A, B and C (see figure 5) that is symmetric under the interchange of phases A and C, with the interfacial tension identifications $\gamma_\mathrm{AC} = 2\gamma_\mathrm{sv}$, $\gamma_\mathrm{AB} = \gamma_\mathrm{BC} = \gamma$ and $\gamma_\mathrm{sl} = 0$. Note that B ('liquid') is the wetting phase. The form (7) guarantees that the proper background surface free energies are subtracted for $x \to \pm\infty$ to yield a finite τ for partial wetting and sufficiently short-ranged forces. When the primitive profile $\ell_\mathrm{P}(x)$ is used, there is no contribution to τ in the homogeneous thin film (recall $V(\ell_1) = 0$), so that the integral effectively starts at $x = x_\mathrm{d}$. Using Young's law

$$\gamma_\mathrm{sv} = \gamma_\mathrm{sl} + \gamma\cos\theta, \quad (8)$$

we arrive at

$$\hat{\tau}[\ell_\mathrm{P}] = \int_{x_\mathrm{d}}^{\infty} \mathrm{d}x \, \{\tfrac{1}{2}\gamma\tan^2\theta + V_S(\ell_\mathrm{P}(x)) - \gamma[1/\cos\theta - \cos\theta]\}, \quad (9)$$

where the subscript P refers to the primitive profile. Note that it is only the profile $\ell(x)$, and not $V_S(\ell)$, that is being approximated in (9). Since, in the small angle approximation, we keep terms up to second order in θ only, and since

$$V_S(\infty) \equiv -S \approx \gamma\theta^2/2, \quad (10)$$

we obtain

$$\hat{\tau}[\ell_\mathrm{P}] = \int_{x_\mathrm{d}}^{\infty} \mathrm{d}x \, \{V_S(\ell_\mathrm{P}(x)) - V_S(\infty)\}. \quad (11)$$

3.2. First-order wetting

When approaching a first-order wetting transition the thin film remains microscopic and ultimately coexists with a macroscopic wetting layer, as $\theta \to 0$. The primitive profile is not well suited to accommodate the transition zone between film and layer, because it converges to a more and more flat profile (almost) independent of x. The piecewise linear approximation $\ell_\mathrm{P}(x)$ is therefore a rather poor approximation to the optimal profile (figure 7). Let us analyze the line tensions associated with both in some detail.

At first sight one might think that for the primitive profile $\tau_\mathrm{P} \to 0$ for $\theta \to 0$, since seemingly the contact line gradually disappears. But, no matter how small the contact angle, the profile must still connect the thin film to the macroscopic layer. Thus, while the profile flattens, the transition zone widens!

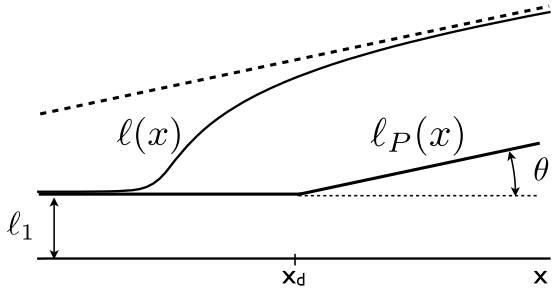

Figure 7. Qualitative comparison of the two interface displacement profiles approaching a first-order wetting transition: (top) optimal profile $\ell(x)$; (bottom) primitive, piecewise linear profile $\ell_\mathrm{P}(x)$. The contact angle θ is the same for both configurations. The dividing line lies at $x = x_\mathrm{d}$ for the primitive profile. For the optimal profile the dividing line is far to the left (outside the picture) where the dashed line intersects the line $\ell = \ell_1$. For clarity the dividing lines have been shifted relative to one another.

Using (11) we obtain

$$\hat{\tau}[\ell_\mathrm{P}] = \int_{x_\mathrm{d}}^{\infty} \frac{\mathrm{d}x}{\mathrm{d}\ell}\{V_S(\ell) - V_S(\infty)\}\,\mathrm{d}\ell = \frac{1}{\tan\theta}\int_{\ell_1}^{\infty}\{V_S(\ell) - V_S(\infty)\}\,\mathrm{d}\ell. \quad (12)$$

We recall that the interface potential $V_{(S=0)}(\ell)$ features a barrier between two equal minima (at first-order wetting), so that, for $\theta \to 0$,

$$\tau_\mathrm{P}(\theta) \equiv \hat{\tau}[\ell_\mathrm{P}] \approx \frac{1}{\theta}\int_{\ell_1}^{\infty} \mathrm{d}\ell \, V_0(\ell). \quad (13)$$

Note how strikingly different this result is from the limit $S \to 0$ in (4), the physically correct expression that results when the optimal profile is employed. The important point is that the integrability of $V_0(\ell)$ is crucially stronger than that of $\sqrt{V_0(\ell)}$. Consequently, we shall find that the $1/\theta$ singularity in the approximate line tension $\tau_\mathrm{P}(\theta)$ is very robust or 'universal'.

Interestingly, expression (13), which appears in our context to be only of mathematical significance, since it is associated with the (physically incomplete) primitive picture of the contact line, also exists as a physical result for a different but closely related setting. It is formally identical to the line tension in the IDM of a liquid adsorbed in a planar solid wedge with opening angle θ, and provides the solvation force f_θ for the wedge through $f_\theta = -\partial\tau/\partial\theta$. Although the interface potential $V(\ell)$ is defined differently in the two settings, (13) is basically equivalent to equation (7) in [18].

In the next two subsections we discuss first-order wetting in systems with short-range forces. The first of these subsections is devoted to the results of the IDM while the second deals with the results of a more microscopic density-functional theory.

3.2.1. First-order wetting and short-range forces: interface displacement model. From the result just obtained in (13) we can conclude that for short-range forces (finite integral) the line

tension associated with the primitive profile diverges at first-order wetting in the manner

$$\tau_{\rm P}(\theta) \sim \frac{\lambda V_{\rm max}}{\theta}, \tag{14}$$

with λ a (finite) length and $V_{\rm max} \equiv V_0(\ell_{\rm max})$ the top of the interface potential barrier. Since λ and $V_{\rm max}$ are model-dependent parameters, we do not expect a universal amplitude here. Since for first-order wetting $\theta \propto |T - T_{\rm w}|^{1/2}$, with T the temperature and $T_{\rm w}$ the wetting transition temperature, the $1/\theta$ divergence of $\tau_{\rm P}$ can be reexpressed as

$$\tau_{\rm P}(T) \propto |T - T_{\rm w}|^{-1/2}. \tag{15}$$

How does this divergence arise? Can we understand it geometrically? Consider the primitive profile, being a linear liquid wedge with very small slope, and let the slope, $\tan\theta \approx \theta$, tend to zero, while keeping the height H, to which $\ell(x)$ rises, macroscopic. That is how this profile connects the thin film to the macroscopic layer. The line tension cost of this piecewise linear solution, with $\ell = \ell_1$ for $x < 0$ and $\ell = \theta x$ for $x > 0$, can be evaluated using (9). Surprisingly, the result is unbounded. It is not the gradient contribution which is costly, since it is canceled exactly by the piecewise constant $c(x)$, which is zero for $x < 0$, and for $x > 0$ corresponds to the counterterm for the linear wedge $\ell(x) \approx \theta x$. Instead, the interface potential cost is the important one. Indeed, as $\theta \to 0$, larger and larger intervals Δx are 'spent' at values of ℓ in a finite range $\Delta\ell$ in the vicinity of the potential barrier at $\ell = \ell_{\rm max}$. Thus the potential line energy cost amounts to $V_{\rm max}\Delta\ell/\theta$. This diverges for $\theta \to 0$, even for fixed H. We conclude that the primitive profile leads to a diverging line tension at first-order wetting. Remarkably, the optimal solution, which solves the Euler–Lagrange equation (2), avoids a divergence and renders τ finite, by traversing 'rapidly' (i.e., on a finite interval Δx) the region of film thicknesses where $V(\ell)$ is not small, and at the same time keeping the profile gradient sufficiently small everywhere. This optimal profile takes the form $\ell(x) \propto \log x$ for short-range forces, and $\ell(x) \propto x^{2/(\sigma+1)}$ for algebraically decaying forces. Figure 7 shows a sketch of the two interface displacement profiles we have discussed, the piecewise linear and optimal ones.

3.2.2. First-order wetting and short-range forces: density-functional model. The predictions of the interface displacement model are substantially supported by computations of the line tension in a more microscopic density-functional model of the three-phase contact line in systems with short-range forces [4]. In that model, which features two densities $\rho_1(x, y)$, $\rho_2(x, y)$, and three phases A, B and C, it is possible to define a 'primitive picture' akin to the primitive profile in the IDM. Indeed, one may define a primitive (piecewise linear) density contour in the (x, y)-plane, perpendicular to the contact line, which runs along the z-axis. The primitive picture then results from constraining one particular density contour to be piecewise linear. The resulting core structure of the contact line will be an approximation to the optimal one (found without imposing a constraint). Consequently, the line tension will be an upper bound to the equilibrium line tension. The contour plots in figure 8 define and illustrate the primitive picture, while the contour plots in figure 5(b) display the optimal core structure.

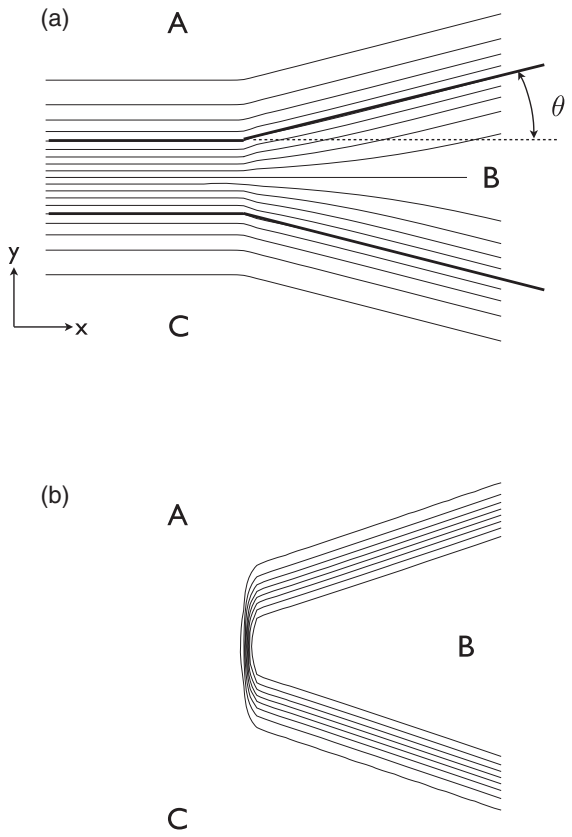

Figure 8. Density contour plots associated with the primitive picture of the contact line in the density-functional model. The two densities ρ_1 and ρ_2 assume the following asymptotic values in bulk: $\rho_1 = -1$ and $\rho_2 = 0$ in phase A, $\rho_1 = 0$ and $\rho_2 = b$ in phase B, $\rho_1 = 1$ and $\rho_2 = 0$ in phase C. (a) Contour plots of the density $\rho_1(x, y)$ subject to the constraint that two contours ($\rho_1 = -1/2$ and $\rho_1 = 1/2$, thick lines) are piecewise linear; (b) contour plots of the density $\rho_2(x, y)$ subject to the same constraint imposed on $\rho_1(x, y)$.

The computation has been performed for the model that features a first-order wetting transition, as described in the first paper of [4]. Table 1 shows the numerical results for $\tau_{\rm P}$ and τ as a function of the contact angle θ, which can be calculated from the distance to the wetting transition as measured by the control variable $b - b_{\rm w}$ employed in the model. As might have been expected based on the IDM prediction, the values of $\tau_{\rm P}$ overestimate the line tension, and the overestimation becomes gross for small θ, eventually entailing a divergence of $\tau_{\rm P}$ proportional to $1/\theta$, in agreement with (13).

These results also explain what had been a puzzling discrepancy between the line tensions calculated by two different methods in an earlier mean-field density-functional model of a first-order wetting transition. In [19], the line tension was evaluated by choosing what appeared to be reasonable functional forms for the spatial variations of the densities of two chemical components, with several adjustable parameters in them, and the variational integral for the line tension was then minimized with respect to those parameters.

Table 1. Line tension as a function of the contact angle θ computed in the density-functional model with two spatially varying densities [4]. The thermodynamic state of the system approaches a first-order wetting transition. The variable $b - b_w$ measures the distance to the wetting point, and $\theta \propto \sqrt{b - b_w}$. The equilibrium line tension is τ, while the line tension associated with the primitive picture of the contact line is τ_P.

$b - b_w$	θ (deg)	τ_P	τ
0.0001	0.734	3.995	0.4484
0.0003	1.229	2.455	0.4273
0.0016	2.796	1.127	0.3745
0.0076	6.068	0.5455	0.2855
0.0196	9.714	0.3259	0.2076

In the first paper of [4], by contrast, for the same model, the spatial variations of the densities were obtained by solving, with high accuracy, the Euler–Lagrange equations for the minimization of the functional integral. Surprisingly, despite the large number of adjustable parameters in the first method, the resulting line tension, as compared with that obtained by the second method, became progressively too high as the contact angle in the wetting phase decreased toward zero and even appeared to diverge at the wetting transition. That the variational approximation would overestimate the line tension was as expected; the surprise was by how much it was overestimated. In retrospect, one can see that the invented functional forms for the spatial variations of the densities in [19] were diffuse versions of the present figure 5(a), not of (b); i.e., they did not make allowance for the deviations of the interfaces near the contact line that we have now seen to be essential for a realistic picture of the contact region near a first-order wetting transition and for correct values of the line tension.

3.2.3. First-order wetting and long-range forces. We now consider the result (13) but in the presence of intermolecular pair potentials in space dimension d with algebraic decay $r^{-(d+\sigma)}$ at large separation r, leading to a power-law behavior of $V_0(\ell)$,

$$V_0(\ell) \propto \ell^{-(\sigma-1)}, \qquad \text{for large } \ell. \tag{16}$$

We conclude that the amplitude of $1/\theta$ is finite provided $\sigma > 2$. This means that for van der Waals forces ($\sigma = 3$) or retarded van der Waals forces ($\sigma = 4$) the line tension for the primitive profile will show the same divergence, $1/\theta$, as for short-range forces. We recall that for $\sigma \leqslant 2$ the line tension is already positive infinity in the partial wetting regime (at finite θ) [10] and therefore the upper bound τ_P is necessarily infinite too.

If we compare this result

$$\tau_P(\theta) \propto 1/\theta \tag{17}$$

with those for the optimal profiles [10] we observe that the primitive profile leads to a qualitative overestimation of the line tension, for all σ, since for optimal profiles

$$\begin{aligned} \tau(\theta) - \tau(0) &\propto \theta^{(\sigma-3)/(\sigma-1)}, \qquad \text{for } \sigma > 3 \\ \tau(\theta) &\propto \theta^{-(3-\sigma)/(\sigma-1)}, \qquad \text{for } 2 < \sigma < 3 \end{aligned} \tag{18}$$

which is either finite at wetting ($\tau(0) > 0$ for $\sigma > 3$) or diverges with a non-universal exponent that is always greater than -1 for $2 < \sigma \leqslant 3$. In particular, recall the interesting case of van der Waals forces ($\sigma = 3$) for which $\tau(\theta) \propto \log(1/\theta)$.

3.3. Critical wetting

Approaching a critical wetting transition we also arrive at

$$\hat{\tau}[\ell_P] \sim \frac{1}{\theta} \int_{\ell_1}^{\infty} \mathrm{d}\ell \; V_0(\ell), \qquad \text{for } \theta \to 0, \tag{19}$$

but we now face the situation that $\ell_1 \to \infty$ for $\theta \to 0$. That is, the interface potential possesses a single minimum which gradually moves out to infinity. Therefore, we may anticipate that the integral in (19) vanishes, which may overrule the diverging prefactor $1/\theta$.

Firstly, note that $\tau_P \leqslant 0$, since $V_S(\ell) \leqslant V_S(\infty)$ due to the absence of a barrier in $V_S(\ell)$. This can easily be verified by inspecting the form (12) which also holds close to a critical wetting transition. Incidentally, the line tension for the optimal profiles near critical wetting is also negative [10]. Thus we expect that τ_P will tend to zero at critical wetting in most cases of interest since τ_P is an upper bound to τ and since τ typically vanishes at critical wetting (unless the forces are very long ranged). This leads us to suspect that, unlike for first-order wetting, τ_P may be a reasonable approximation to τ.

If, indeed, τ_P tends to zero, then it must be so that $\int_{\ell_1}^{\infty} \mathrm{d}\ell \; V_0(\ell)$ vanishes faster than θ for $\theta \to 0$. Let us now investigate this.

3.3.1. Critical wetting and short-range forces. Consider the model [10]

$$V_S(\tilde{\ell}) = A\mathrm{e}^{-\tilde{\ell}} + B\mathrm{e}^{-2\tilde{\ell}} - S, \tag{20}$$

where $\tilde{\ell}$ is dimensionless; e.g., $\tilde{\ell} = \ell/\xi$, with ξ the bulk correlation length in the 'liquid' phase. As usual, let $A \propto T - T_{cw}$, with T_{cw} the critical wetting temperature. We have $A < 0$ for partial wetting and $\theta \propto T - T_{cw}$. Recall also $-S \approx \gamma\theta^2/2$. The equilibrium film thickness was found to be $\tilde{\ell}_1 = \log(2B/|A|)$ and the normalization of V_S implies the following identity:

$$V_S(\tilde{\ell}_1) = -\frac{|A|^2}{4B} - S = 0. \tag{21}$$

We now find by means of (12)

$$\hat{\tau}[\ell_P] = -\frac{3}{8}\frac{\xi}{\tan\theta}\frac{|A|^2}{B} \sim -\frac{3}{4}\xi\gamma\theta, \tag{22}$$

which is a universal result in the sense that there are no remaining model-dependent parameters like the ratio B/A_0, with $A = A_0(T - T_{cw})$, for example, and gives us confidence that a somewhat different choice of model will yield the same result.

It is interesting to compare this upper bound τ_P with the previously obtained [10, 20] optimal τ, being

$$\tau(\theta) = -\xi\gamma\theta, \tag{23}$$

as was calculated using (4). We conclude that the upper bound satisfies, for $\theta \to 0$,

$$\frac{\tau_{\rm P}}{\tau} = \frac{3}{4}, \qquad \text{and} \qquad \tau_{\rm P}, \tau < 0. \tag{24}$$

In the light of the questions asked in our section 2 this means that in this case (critical wetting and short-range forces) the contribution of interface deviations near the contact line to the line tension is precisely one quarter of the total amount.

3.3.2. Critical wetting and long-range forces. Consider the model [10]

$$V_S(\tilde{\ell}) = A\tilde{\ell}^{-(\sigma-1)} + B\tilde{\ell}^{-\sigma} - S. \tag{25}$$

As usual, let $A \propto T - T_{\rm cw}$, with $T_{\rm cw}$ the critical wetting temperature. We have $A < 0$ for partial wetting and $\theta \propto (T - T_{\rm cw})^{\sigma/2}$. Recall also $-S \approx \gamma\theta^2/2$. The equilibrium film thickness was found to be $\tilde{\ell}_1 = -(\sigma/(\sigma-1))B/A$ and the normalization of V_S implies the following identity:

$$V_S(\tilde{\ell}_1) = -\frac{1}{\sigma}\left(\frac{\sigma-1}{\sigma}\right)^{\sigma-1}\frac{|A|^\sigma}{B^{\sigma-1}} - S = 0. \tag{26}$$

Then we calculate

$$\begin{aligned}\hat{\tau}[\ell_{\rm P}] &= \frac{\xi}{\tan\theta}\int_{\tilde{\ell}_1}^{\infty} {\rm d}\tilde{\ell}\,(V_S(\tilde{\ell}) + S)\\ &= -\frac{\xi}{\tan\theta}\left(\frac{1}{\sigma-2} - \frac{1}{\sigma}\right)\left(\frac{\sigma-1}{\sigma}\right)^{\sigma-2}\frac{|A|^{\sigma-1}}{B^{\sigma-2}}\\ &= -\frac{\xi\gamma}{\tan\theta}\frac{1}{(\sigma-2)}\left(\frac{1}{\sigma-1}\right)^{1/\sigma}\left(\frac{2B}{\gamma}\right)^{1/\sigma}\theta^{1+(\sigma-2)/\sigma}\\ &\propto \theta^{(\sigma-2)/\sigma}.\end{aligned} \tag{27}$$

This is to be compared with the known result for the optimal profile

$$\tau = -K(\sigma,2)\xi\gamma\left(\frac{2B}{\gamma}\right)^{1/\sigma}\theta^{(\sigma-2)/\sigma}, \tag{28}$$

with $K(\sigma,2)$ a well-defined σ-dependent coefficient [20].

Note that the same singularity is found for $\tau_{\rm P}$ as for τ. The amplitudes differ, but typically only by about 20%. For example, recalling $\tau_{\rm P}, \tau < 0$,

$$\begin{aligned}\frac{\tau_{\rm P}}{\tau} &\approx 0.83, \qquad \text{for } \sigma = 3,\\ \frac{\tau_{\rm P}}{\tau} &\approx 0.81, \qquad \text{for } \sigma = 4,\end{aligned} \tag{29}$$

where use was made of the numerical values $K(3,2) \approx 0.95$ and $K(4,2) \approx 0.47$ [20]. In line with the conclusion of the subsection on critical wetting and short-range forces, we find that in this case (critical wetting and long-range forces of van der Waals or similar type) the contribution of interface deviations near the contact line to the line tension is approximately one fifth of the total amount.

3.4. Multicritical wetting

We now generalize our results for critical wetting to multicritical wetting transitions, in the same spirit as the earlier generalization of the line tension investigation to multicritical wetting [20].

3.4.1. Multicritical wetting and short-range forces. Consider the model [20], a generalization of (20),

$$V_S(\tilde{\ell}) = A{\rm e}^{-\tilde{\ell}} + Y_n{\rm e}^{-n\tilde{\ell}} - S. \tag{30}$$

In this model, for $A \to 0$ we approach nth order wetting criticality; $n = 2$ for critical, $n = 3$ for tricritical wetting, etc. As usual, let $A \propto T - T_{\rm mcw}$, with $T_{\rm mcw}$ the multicritical wetting temperature. We have $A < 0$ for partial wetting and $\theta \propto |T - T_{\rm mcw}|^{n/(2(n-1))}$. Recall also $-S \approx \gamma\theta^2/2$. The equilibrium film thickness was found to be $\tilde{\ell}_1 = (1/(n-1))\log(nY_n/|A|)$ and the normalization of V_S implies the following identity:

$$V_S(\tilde{\ell}_1) = (-n^{-1/(n-1)} + n^{-n/(n-1)})|A|^{n/(n-1)}Y_n^{-1/(n-1)} - S = 0. \tag{31}$$

We now find by means of (12)

$$\begin{aligned}\hat{\tau}[\ell_{\rm P}] &= -(n^{-1/(n-1)} - n^{-(2n-1)/(n-1)})\\ &\quad\times\frac{\xi}{\tan\theta}|A|^{n/(n-1)}Y_n^{-1/(n-1)}\\ &= -\left(\frac{n+1}{2n}\right)\gamma\xi\,\theta\end{aligned} \tag{32}$$

which generalizes the 'universal' result (22) found for critical wetting to multicritical wetting.

It is interesting to compare this upper bound $\tau_{\rm P}$ with the previously calculated optimal τ, being

$$\tau(\theta) = -J(n)\gamma\xi\,\theta, \tag{33}$$

with $J(n)$ a well-defined n-dependent coefficient [20].

We recall some numerical values [20] $J(2) = 1$, $J(3) \approx 0.88, \ldots$, $J(\infty) \approx 0.61$. As is easily verified using (32), our present upper bound approximates these amplitudes by 3/4 for $n = 2$ (critical), 2/3 for $n = 3$(tricritical), $\ldots$, 1/2 for $n = \infty$. We conclude that for short-range forces the quality of the primitive-profile approximation to the line tension (slightly) improves with increasing order of multicriticality n.

3.4.2. Multicritical wetting and long-range forces. Consider the model [20]

$$V_S(\tilde{\ell}) = A\tilde{\ell}^{-(\sigma-1)} + Y_n\tilde{\ell}^{-(\sigma+n-2)} - S. \tag{34}$$

As usual, let $A \propto T - T_{\rm mcw}$, with $T_{\rm mcw}$ the multicritical wetting temperature. We have $A < 0$ for partial wetting and $\theta \propto |T - T_{\rm cw}|^{(\sigma+n-2)/2(n-1)}$. Recall also $-S \approx \gamma\theta^2/2$. The equilibrium film thickness was found to be

$$\tilde{\ell}_1 = \left[\left(\frac{\sigma+n-2}{\sigma-1}\right)\frac{Y_n}{|A|}\right]^{1/(n-1)} \tag{35}$$

and the normalization of V_S implies the identity

$$\begin{aligned}V_S(\tilde{\ell}_1) = -\Bigg[&\left(\frac{\sigma-1}{\sigma+n-2}\right)^{(\sigma-1)/(n-1)}\\ &-\left(\frac{\sigma-1}{\sigma+n-2}\right)^{(\sigma+n-2)/(n-1)}\Bigg]\\ &\times|A|^{(\sigma+n-2)/(n-1)}Y_n^{-(\sigma-1)/(n-1)} - S = 0.\end{aligned} \tag{36}$$

Finally we calculate

$$\hat{\tau}[\ell_{\rm P}] = \frac{\xi}{\tan\theta}\int_{\tilde{\ell}_1}^{\infty} {\rm d}\tilde{\ell}\,(V_S(\tilde{\ell}) + S)$$
$$= -\frac{1}{2}\left(\frac{\sigma+n-2}{(\sigma-1)(\sigma-2)} - \frac{1}{\sigma+n-3}\right)$$
$$\times \left(\frac{\sigma-1}{n-1}\right)^{(\sigma+n-3)/(\sigma+n-2)} \xi\gamma\left(\frac{2Y_n}{\gamma}\right)^{1/(\sigma+n-2)} \theta^{\psi}, \quad (37)$$

where the critical exponent ψ depends on σ and n through

$$\psi = \frac{\sigma+n-4}{\sigma+n-2}. \quad (38)$$

Comparison with the exact results obtained in [20] teaches us that $\tau_{\rm P}$ and τ differ only in their numerical prefactors. The critical exponent ψ and also the exponent $1/(\sigma+n-2)$ of $2Y_n/\gamma$ are the same in both. Further comparison of the amplitudes reveals that, e.g., for tricritical wetting ($n = 3$) the upper bound and the exact value differ by about 20%, which is similar to what we already found for critical wetting (corresponding to $n = 2$ here). Specifically, we obtain the approximation $-5/6$ to the exact amplitude -1 for $\sigma = 3$ and $n = 3$, and the approximation -0.40 to the exact amplitude $-0.505\ldots$ for $\sigma = 4$ and $n = 3$. We conclude that for long-range forces the quality of the primitive-profile approximation to the line tension does not change noticeably with increasing order of multicriticality n.

4. Conclusion

In this paper we have investigated how important the core structure of the three-phase contact line is for the line tension in the vicinity of a wetting phase transition. By core structure we mean the deviations of the interfaces away from simple intersecting planes. The geometrical structure in which three planar interfaces intersect in a single common line is termed the 'primitive picture'. We have calculated the line tension associated with the primitive picture analytically, using the simple interface displacement model and—for the case of first-order wetting—also numerically, using a density-functional theory with two spatially varying densities and three phases. We have compared the results with known 'exact' results (within mean-field theory) based on relaxed (equilibrium) profiles that feature the suitable interface deviations. Naturally, the line tension associated with the primitive profile is an upper bound to the true line tension calculated in previous works.

Surprisingly, the quality of the upper bound to the line tension derived using the primitive profile depends crucially on the order of the wetting transition. If the wetting transition is of first order the primitive profile leads to a huge overestimation of the line tension, because the primitive profile totally misses the interesting and important structure of the transition zone between the thin film and the macroscopic wetting layer at wetting. Incidentally, this explains the discrepancy between the line tensions calculated by two different methods in an earlier density-functional model for first-order wetting (section 3.2.2). On the other hand, if the wetting transition is critical (or multicritical) the primitive profile is surprisingly adequate and its line tension is in full qualitative agreement with the exact (mean-field) one. In that case the discrepancy between the upper bound and true value is at most 25%.

Whereas the order of the wetting transition is all-important for the line tension associated with the primitive picture we focused on in this work, the range of the intermolecular forces is much less influential. Indeed, for first-order wetting the primitive profile leads to a robust $1/\theta$ divergence of the line tension (θ being the thermodynamic contact angle that vanishes at wetting), largely regardless of the range of the forces. In contrast, the true (mean-field) line tension at first-order wetting is very sensitive to the range of the forces, remaining finite for short-range forces and diverging for forces of long range (non-retarded van der Waals forces being the borderline case). For critical wetting the influence of the range of the forces is of less concern, since typically the line tension vanishes, in a manner determined by the range of the forces, which is captured qualitatively correctly by the theory whether or not the primitive-profile approximation is employed.

All the results discussed in this work were derived within mean-field theories and their validity is therefore limited. The discussion of the line tension at wetting beyond mean-field theory has been the subject of various papers [21–23], but falls outside our present scope.

Acknowledgments

The authors are pleased and honored to have participated in this tribute to Henk Lekkerkerker, who has been a continual inspiration to all workers in this field. The problem of the structure of interfaces in phase equilibrium has interested Henk for many years, which makes it a special pleasure to dedicate this contribution to him. JOI wishes to express his deep gratitude to Henk for his advice on problems in soft condensed matter physics and chemistry, as well as for his support and friendship, which he has enjoyed already for three decades. KK and BW echo these sentiments. Much of this work was done while JOI was a visitor in the home universities of his co-authors.

References

[1] Aarts D G A L, Dullens R P A, Lekkerkerker H N W, Bonn D and van Roij R 2004 *J. Chem. Phys.* **120** 1973
Lekkerkerker H N W, de Villeneuve V W A, de Folter J W J, Schmidt M, Hennequin Y, Bonn D, Indekeu J O and Aarts D G A L 2008 *Eur. Phys. J.* B **64** 341
Hennequin Y, Aarts D G A L, Indekeu J O, Lekkerkerker H N W and Bonn D 2008 *Phys. Rev. Lett.* **100** 178305
Hennequin Y, Aarts D G A L, Indekeu J O, Lekkerkerker H N W and Bonn D 2010 *Phys. Rev.* E **81** 041604
[2] Rowlinson J S and Widom B 2002 *Molecular Theory of Capillarity* (New York: Dover)
[3] For a recent review, see Bonn D, Eggers J, Indekeu J O, Meunier J and Rolley E 2009 *Rev. Mod. Phys.* **81** 739
[4] Koga K and Widom B 2007 *J. Chem. Phys.* **127** 064704
Koga K and Widom B 2008 *J. Chem. Phys.* **128** 114716
[5] Schimmele L, Napiorkowski M and Dietrich S 2007 *J. Chem. Phys.* **127** 164715

[6] Amirfazli A and Neumann A W 2004 *Adv. Colloid Interface Sci.* **110** 121
[7] Indekeu J O 1994 *Int. J. Mod. Phys.* B **8** 309
[8] Bauer C and Dietrich S 1999 *Eur. Phys. J.* B **10** 767
Koch W, Dietrich S and Napiorkowski M 1995 *Phys. Rev.* E **51** 3300
[9] Indekeu J O 2010 *Physica* A **389** 4332
[10] Indekeu J O 1992 *Physica* A **183** 439
[11] Blokhuis E 1994 *Physica* A **202** 402
[12] Dobbs H T and Indekeu J O 1993 *Physica* A **201** 457
[13] For a review, see Fisher M E 1986 *J. Chem. Soc. Faraday Trans.* II **82** 1569
[14] de Feijter J A and Vrij A 1972 *J. Electroanal. Chem.* **37** 9
[15] Gibbs J W 1928 *The Collected Works of J. Willard Gibbs* vol 1 (New York: Longmans Green) pp 287–8
[16] For various types of core structures, see figure 3 in de Gennes P-G 1985 *Rev. Mod. Phys.* **57** 827
[17] Joanny J-F and de Gennes P-G 1986 *J. Colloid Interface Sci.* **111** 94
[18] Henderson J R 2002 *Physica* A **305** 381
[19] Szleifer I and Widom B 1992 *Mol. Phys.* **75** 925
[20] Indekeu J O, Backx G and Langie G 1993 *Physica* A **196** 335
[21] Indekeu J O and Robledo A 1993 *Phys. Rev.* E **47** 4607
[22] Abraham D B, Latrémolière F T and Upton P J 1993 *Phys. Rev. Lett.* **71** 404
[23] Parry A O, Greenall M J and Wood A J 2002 *J. Phys.: Condens. Matter* **14** 1169